

# Studying subthreshold resonance using the Trojan horse method

Xue-Jian Wang,<sup>1</sup> Qun-Gang Wen,<sup>1,\*</sup> Cheng-Bo Li,<sup>2,†</sup> and Jian-You Guo<sup>1,‡</sup>

<sup>1</sup>*School of Physics and Materials Science, Anhui University, Hefei 230601, China*

<sup>2</sup>*Institute of Radiation Technology, Beijing Academy of Science and Technology, Beijing 1000875, China*

(Dated: September 13, 2023)

The Trojan horse method was employed to indirectly measure the bare-nucleus reaction cross-section and astrophysical S-factor of the  ${}^9\text{Be}(p,\alpha){}^6\text{Li}$  reaction in the low-energy region, utilizing the three-body reaction  ${}^2\text{H}({}^9\text{Be},\alpha){}^6\text{Li}$ n. Comparing the two-body reaction data extracted from the Trojan horse method with that obtained through direct measurements, compatibility is observed in the energy region above approximately 100 keV. Additionally, the THM data successfully reproduces the expected low-energy resonance peak around 270 keV. The THM extraction of the astrophysical factor yields  $S(0) = 21.0 \pm 0.8$  MeV b, which surpasses the extrapolation obtained from direct measurements. The  ${}^9\text{Be}(p,\alpha){}^6\text{Li}$  reaction channel exhibits a subthreshold resonance with a width of 25 keV, positioned approximately -23 keV below the threshold. However, the strong electron shielding effect near the zero energy position in direct measurements often masks the influence of the subthreshold resonance on the low-energy region. In contrast, the THM method allows us to neglect the electron shielding effect. The THM experimental data were subjected to fitting using the Breit-Wigner function and subsequently compared with directly measured data. Following a comprehensive comparative analysis, it was discerned that the  $S(0)$  value obtained through THM exceeded the extrapolated value derived from direct measurements. This disparity was primarily attributed to the influence of the subthreshold resonance.

PACS numbers: 24.50.+g, 24.10.-i, 25.70.Hi, 26.20.-f

## I. INTRODUCTION

Research on the abundance of light elements Li, Be, and B is of paramount importance in the field of nuclear astrophysics. The primordial abundance of light nuclei is considered a crucial parameter for testing the accuracy of models of non-uniform primordial nucleosynthesis in the context of the Big Bang theory [1–3]. Additionally, it serves as a precise probe for the internal mechanisms of stars [4–6]. The dominant process for destroying  ${}^9\text{Be}$  in astrophysical environments occurs through the proton-initiated (p, $\alpha$ ) reaction channel. Measurement of the bare-nucleus reaction cross sections for  ${}^9\text{Be}(p,\alpha){}^6\text{Li}$  is essential in the astrophysical energy range of 10–100 keV [7, 8]. This energy range lies below the Coulomb barriers, and nuclear reactions can only occur through barrier penetration effects. As a result, the reaction cross-section decreases exponentially with decreasing energy. Experimental measurements of nuclear reactions in such a low energy range are challenging [9–11]. To facilitate extrapolation, the concept of the astrophysical S-factor is introduced, which exhibits minimal sensitivity to energy variation [12]:

$$S(E) = E[\sigma(E)]\exp(2\pi\eta) \quad (1)$$

$$\eta = \frac{Z_1 Z_2 e^2}{\hbar v} = Z_1 Z_2 \alpha \left( \frac{\mu c^2}{2E} \right)^{1/2} \quad (2)$$

In Eq.(2)  $\eta$  is the Sommerfeld parameter,  $Z_1, Z_2$  are the charge numbers of the two particles,  $\mu$  and  $E$  are the approximate mass and energy of the center-of-mass system,  $\alpha = 1/137$  is the refinement structure constant, and  $c$  represents the speed of light. The reaction cross section can be expressed as Eq.(3):

$$\sigma(E) = S(E)E^{-1}\exp(-2\pi\eta) \quad (3)$$

The cross section can be divided into three components. Firstly,  $S(E)$  characterizes the contribution of purely nuclear interactions to the cross section. In the absence of resonances, it exhibits a gentle variation with energy. Secondly,  $E^{-1}$  is a non-nuclear factor associated with the de Broglie wavelength. Lastly, the Gamow factor,  $\exp(-2\pi\eta)$ , characterizes the probability of Coulomb barrier penetration and plays a crucial role in determining the sharp decrease of the reaction cross section with increasing energy.

In recent years, various indirect methods have been developed to mitigate the uncertainties introduced by extrapolation. One such method is the Trojan Horse Method (THM) [11, 13]. The Trojan Horse Method is founded on the principles of quasi-free reactions and operates under specific kinematic conditions. It selects a three-body reaction closely related to a two-body reaction under consideration. This three-body reaction occurs above the Coulomb barrier, thus avoiding the inhibiting effect of the Coulomb barrier on cross-sections. Additionally, electron screening effects can be negligibly small in this context. The first experimental measurement of the electron screening potential was conducted by Engstler and colleagues in 1988 through the study of the  ${}^3\text{He}(d,p){}^4\text{He}$  reaction. Subsequently, researchers have explored the electron screening potential through a series

\*E-mail: qungang@ahu.edu.cn

†E-mail: lichengbo@brc.ac.cn

‡E-mail: jianyong@ahu.edu.cn

of nuclear reaction experiments. The results consistently indicate that electron screening effects in low-energy nuclear reactions lead to anomalously increased reaction cross-sections and S-factor [14–16].

Utilizing the Trojan Horse Method to investigate charged particles reactions in the astrophysical energy regime enables researchers to overcome the challenges posed by electron screening effects and the Coulomb barrier in direct measurements. In the  ${}^9\text{Be}(p,\alpha){}^6\text{Li}$  reaction channel, there exists a sub-threshold resonance with a width of approximately 25 keV at energies around -23 keV [17]. Combining the bare-nucleus reaction data obtained through the Trojan Horse Method with direct measurement data, followed by further analysis, can greatly contribute to our understanding of the influence of sub-threshold resonances on reaction cross-sections in the astrophysical energy range.

## II. TROJAN HORSE METHOD

The Trojan horse method (THM) is an indirect measurement [18–20] that utilizes a quasi-free reaction mechanism to extract the dependence of the astrophysical factor  $S(E)$  of the astrophysically relevant two-body reaction with energy through the associated three-body reaction. As shown in Fig. 1, this method is applicable to charged particle two-body reactions of astrophysical interest:

$$A + x \rightarrow C + c \quad (4)$$

Select a three-body reaction that is closely related to it:

$$A + a \rightarrow C + c + b \quad (5)$$

The nucleus  $a$  can be viewed as composed of two components,  $x$  and  $b$ , which are loosely bound ( $a = x + b$ ). To ensure appropriate kinematic conditions, the momentum transfer of nucleus  $b$  during the nuclear reaction is chosen to be very small and negligible compared to  $x$ . Consequently, the nuclear reaction can be considered to occur between nucleus  $A$  and  $x$ . The  $b$  nucleus acts as a bystander in the  $A+x$  reaction, with its energy-momentum remaining unchanged, similar to its state in the parent

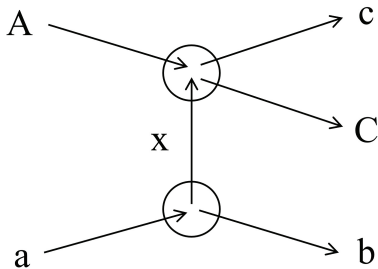


FIG. 1: Diagram of Trojan horse method.

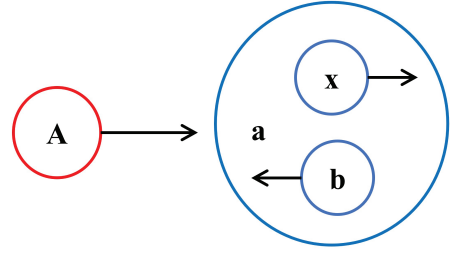


FIG. 2: The Fermi motion of  $x$  in  $a$  leads to a small relative energy of  $A-x$ .

nucleus  $a$ . The component  $x$  is referred to as the Participant of the quasi-free reaction, while  $b$  is called the Spectator of the reaction. The parent nucleus  $a$ , which carries the nucleus  $x$ , is known as the Trojan nucleus. In this experiment, the Trojan nucleus is  ${}^2\text{H}$ , where  ${}^2\text{H} = p + n$ , with the proton acting as the active participant in the nuclear reaction and the neutron acting as a bystander in the two-body reaction  ${}^9\text{Be}(p,\alpha){}^6\text{Li}$ .

After selecting the appropriate Trojan nuclei and three-body reactions, it is also necessary to choose the appropriate incident particle energies. The incident energy ( $E_{Aa}$ ) of the three-body reaction in the quasi-free reaction needs to be partially used to overcome the binding energy of  $x$  in the Trojan nucleus  $a$ . It should be noted that the  $x$  nucleus exhibits a certain momentum distribution in  $A$  (as shown in Fig. 2). When  $x$  and  $A$  are moving in the same direction, their relative motion can be mostly or even completely canceled out. Therefore, even if the relative energy ( $E_{Aa}$ ) of the incident channel  $A-a$  is large, the relative energy ( $E_{Ax}$ ) of the  $A-x$  system can be very small, approaching zero. The choice of incident particle energy should consider several factors. Firstly, the relative energy ( $E_{Aa}$ ) of the  $A-a$  system needs to be above the Coulomb barrier. This ensures that the Coulomb barrier does not cause a sharp decrease in the cross-section, making it difficult to measure the reaction cross-section in the low-energy region. Secondly, it is important to make the relative energy ( $E_{Ax}$ ) of the  $A-x$  system close to zero. This is desired because the cancellation of relative motion between  $A$  and  $x$  allows for a more efficient quasi-free reaction. Therefore, when selecting the energy of the incident channel particles, it is necessary to find a balance between these considerations. The incident energy should be sufficient to overcome the Coulomb barrier and ensure a measurable cross-section, while also allowing for the relative energy of the  $A-x$  system to approach zero, taking into account the momentum distribution of  $x$  in  $a$ .

The energy relationship between two-body and three-body reactions can be obtained from the three-body reaction quasi-free condition and conservation of energy [21]:

$$E_{Ax}^{qf} = E_{Aa} \left( 1 - \frac{\mu_{Aa}}{\mu_{Bb}} \frac{\mu_{bx}^2}{m_x^2} \right) - \varepsilon_a \quad (6)$$

$\varepsilon_a = (m_x + m_b + m_a)c^2$  is the Trojan nuclei's binding energy.  $E_{Ax}$  is the energy interval centered on  $E_{Ax}^{qf}$ :  $E_{Ax} = (E_{Ax}^{qf} - E_{cut}, E_{Ax}^{qf} + E_{cut})$ ,  $E_{cut}$  is the energy cutoff determined by the momentum width of the Fermi motion. Thus corresponding to a beam energy point, two-body reaction data can be obtained for a section of the energy interval near the quasi-free energy point.

The experiment was performed at Beijing Tandem Accelerator National Laboratory, of the China Institute of Atomic Energy. A beam of  $^9\text{Be}$  of 22.35 MeV was provided by the HI-13 tandem accelerator. The beam intensity ranged between 10 and 20 nA [20]. When the beam current of  $^9\text{Be}$  exceeds the Coulomb barrier, the three-body reaction can occur above the barrier, and the two-body reaction takes place in the nuclear interaction region with the assistance of the three-body reaction. The effects of the Coulomb barrier and electron shielding can be neglected. Information regarding the desired two-body reaction is extracted through the three-body reaction  $^2\text{H}(^9\text{Be}(p,\alpha)^6\text{Li})n$ , with complete kinematic measurements of  $\alpha$  and  $^6\text{Li}$ .

### III. DATA ANALYSIS

In this experiment, the bare-nucleus reaction cross section and astrophysical S-factor of the  $^9\text{Be}(p,\alpha)^6\text{Li}$  astronomical nuclear reaction in the low-energy region are indirectly measured using the Trojan horse method. The desired information about the two-body reaction is extracted through the three-body reaction  $^2\text{H}(^9\text{Be}(p,\alpha)^6\text{Li})n$ , with complete kinematic measurements of  $\alpha$  and  $^6\text{Li}$ . The experimental data obtained using the Trojan horse method are listed in Table 1 [20].

TABLE I: Astrophysical S-factor of  $^9\text{Be}(p,\alpha)^6\text{Li}$  reaction channel obtained by Trojan horse method.

$E_{c.m.}/\text{MeV}$	$S(E)/\text{MeV b}$	$\Delta S(E)/\text{MeV b}$
0.0125	20.7	4
0.0375	21.3	4
0.0625	26.3	5
0.0875	30.7	5
0.1125	33.8	5
0.1375	41.6	6
0.1625	51.0	7
0.1875	60.6	8
0.2125	71.9	9
0.2375	84.6	10
0.2625	91.7	11
0.2875	89.7	11

The experimental data obtained through the Trojan horse method accurately reproduce the expected low-energy resonance peak at  $\sim 270$  keV. These indirect measurements align with the direct measurements in the energy region above approximately 100 keV. However, the direct measurements show a significant increase in the energy region below 100 keV, which can be attributed to the effect of electron shielding potential [20]. Sierk and Tombrello conducted measurements the reaction cross section of this reaction channel. They analyzed the data using R-matrix method that incorporated three broad resonances. The results approximately replicated the structure observed in the data [22]. Notably, the data exhibit a decreasing trend towards lower energies in the  $E_p \leq 100$  keV energy region, reaching a minimum in  $S(E)$  followed by a steep rise. Further measurements of this reaction channel and the reaction cross-section were conducted by Zahnow et al. within the energy range of  $E_p = 16$  to 390 keV [23]. When compared to the results of Sierk et al., the two sets of measurements show greater consistency in the energy region of  $E_p > 100$  keV, but significant differences emerge below 100 keV. The increasing trend at the low-energy end is influenced by both the subthreshold resonance and the electron shielding effect. The direct measurement result by F. Kaihong et al. yields a result of  $S(0) = 16.2 \pm 1.8$  MeV b for the astrophysical factor [24]. In contrast, the Trojan horse method extracts a higher value of  $S(0) = 21.0 \pm 0.8$  MeV b, surpassing the direct measurement extrapolation. The reaction channel has a subthreshold resonance with a width of 25 keV at a subthreshold of about -23 keV. It is speculate that the higher  $S(0)$  obtained through the THM is primarily due to the presence of this subthreshold resonance. To investigate the impact of the subthreshold resonance on the astronomical factor, the Breit-Wigner function is utilized in Fig. 3 to fit the THM data.

$$S(E) = S_0(E) + S_1(E) \quad (7)$$

$$S_0(E) = \frac{A_0 \times (\Gamma_0/2)^2}{(E - E_0)^2 \times (\Gamma_0/2)^2} \quad (8)$$

$$S_1(E) = \frac{A_1 \times (\Gamma_1/2)^2}{(E - E_1)^2 \times (\Gamma_1/2)^2} \quad (9)$$

Eq.(7) is the Breit-Wigner function. Two Gaussian peaks,  $S_0(E)$  Eq.(8) and  $S_1(E)$  Eq.(9), fit the data extracted from the THM indirect measurements. The suprathreshold energy peak was fitted using  $S_0(E)$ , while the subthreshold resonance peak was fitted using  $S_1(E)$  with an  $E_1$  of -23 keV. The individual parameters of the fit are shown in Table II.

Fig. 3 illustrates the comparison between the THM data fit using the Breit-Wigner function and the direct measurement of the fitted data. In Fig. 3 the THM-extracted astronomical factor  $S(E)$  data points [20] are represented by solid square symbols. The astronomical factor  $S(E)$

TABLE II: Parameters for fitting THM data using the Breit-Wigner function.

$A_0$	$E_0/\text{keV}$	$\Gamma_0/\text{keV}$	$A_1$	$E_1/\text{keV}$	$\Gamma_1/\text{keV}$	$S_0(0)/\text{MeV b}$	$S(0)/\text{MeV b}$
$92 \pm 8$	$279 \pm 33$	$260 \pm 42$	$10 \pm 4$	-23	$48 \pm 73$	16.3	21.5

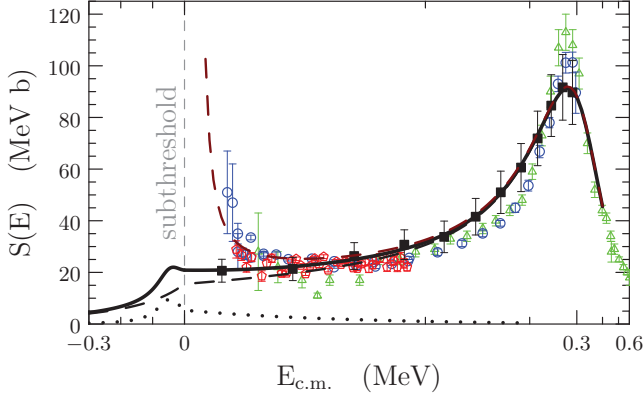


FIG. 3: Breit-Wigner function fitted THM data compared with direct measurement fitted data.

data points from direct measurements [22], [23], and [24] are denoted by hollow triangles, hollow circles, and hollow pentagons, respectively. The red dashed line represents the fitted curve of the directly measured data, taking into account the electron shielding potential. The solid black line corresponds to the THM data fitted using the Breit-Wigner function. This fitted curve exhibits two energy peaks, one above and one below the threshold. The black dashed line represents the fitted suprathreshold energy peak  $S_0(E)$  obtained from the Breit-Wigner function, while the black dotted line corresponds to the fitted subthreshold resonance peak  $S_1(E)$ .

Table II presents the parameters of the THM data fit using the Breit-Wigner function. It is observed that when the effect of subthreshold resonance is not considered,  $S_0(0) = 16.3 \text{ MeV b}$ , which is the same as the direct measurement extrapolation result  $S(0) = 16.2 \pm 1.8 \text{ MeV b}$ . However, when the subthreshold resonance effect is considered,  $S(0) = 21.5 \text{ MeV b}$ , indicating a higher value compared to the direct measurement extrapolation. Examining Fig. 3, we observe that the red dashed line, solid black line, and black dashed line data are consistent in the region above approximately 100 keV. Additionally, there is a pronounced upward trend for the red dashed line in the energy region below 100 keV, attributed to the electron shielding potential effect. Analyzing the data in Fig. 3 in conjunction with Table II, the higher  $S(0)$  obtained by THM than extrapolated from direct measurements is mainly due to subthreshold resonance.

The astrophysical factor  $S_b(E)$  of the bare-nucleus is measured using the Trojan horse method. By comparing  $S_b(E)$  with the directly measured astrophysical factor  $S_d(E)$ , which includes the electron shielding effect, the

electron shielding potential  $U_e$  can be extracted. This can be done using Eq.(10):

$$S_d(E) = S_b(E) \exp\left(\frac{\pi\eta U_e}{E}\right) \quad (10)$$

The astronomical factor  $S_d(E)$  used in the calculation was selected from the direct measurements conducted by Sierk [22], Zahnow [23], and F. Kaihong [24]. By applying Eq.(10), we determined the electron shielding potential as  $U_e = 474 \pm 81 \text{ eV}$ . This value agrees with the electron shielding potential of  $U_e = 545 \pm 98 \text{ eV}$  obtained from direct measurements by F. Kaihong et al. [24]. However, it is lower than the average value of the electron shielding potential [12],  $U_e = 788 \pm 70 \text{ eV}$ , derived from THM [20] and Zahnow [23]. The ratio of the electron shielding potential  $U_e = 474 \pm 81 \text{ eV}$  to the theoretical  $U_e \approx 240 \text{ eV}$  obtained through the atomic model is  $1.97 \pm 0.33$ . It is worth noting that the ratio of the experimental electron shielding potential value for other reaction channels to the theoretical value obtained through the atomic model is also around 2 [12]. This consistency lends further support to the accuracy of the electron shielding potential results obtained in our study.

#### IV. RESULTS AND DISCUSSION

Combining the THM obtained bare-nucleus reaction data with direct measurement data is of paramount importance for a more profound investigation into the influence of sub-threshold resonances on astrophysical reaction cross-sections. Typically, electron screening effects in direct measurement data can obscure the impact of sub-threshold resonances on low-energy region cross-sections. However, employing the THM method allows us to effectively circumvent these electron screening effects. In this study, we utilized the Breit-Wigner function as an analytical tool to handle the THM data. Specifically, we fitted the data with  $S_0(E)$  for the resonance peak above the threshold and employed  $S_1(E)$  to fit the resonance peak below the threshold. Through a comprehensive fitting analysis, we observed that, when do not consider the influence of sub-threshold resonances, the obtained  $S_0(0) = 16.3 \text{ MeV b}$ , which aligns with the results extrapolated from direct measurements. However, when accounting for the impact of sub-threshold resonances, we found that the  $S(0) = 21.5 \text{ MeV b}$ , which exceeded the extrapolated results from direct measurements. The fitting outcomes unambiguously demonstrated that the higher value of  $S(0)$  obtained with the THM method is

primarily attributed to the presence of sub-threshold resonances. Furthermore, through a comparative analysis between THM and direct measurement data, we successfully extracted the electron screening potential,  $U_e = 474 \pm 81$  eV. This value, when compared to the theoretically estimated  $U_e \simeq 240$  eV based on atomic models, yields a ratio of  $1.97 \pm 0.33$ .

In summary, in the study of reaction cross-sections within the astrophysical energy regime, considering the influence of sub-threshold resonances is crucial, as it can significantly impact the measured cross-section values. Additionally, our extraction of the electron screening

potential provides valuable insights for a deeper understanding of bare-nucleus reactions.

### Acknowledgments

This work was supported by the National Natural Science Foundation of China (12075031), the Beijing Natural Science Foundation (12222022), and the National Natural Science Foundation of China (11935001).

- 
- [1] M. Zadro, et al., Phys. Rev. C. **40**, 181 (1989).
  - [2] R. N. Boydet et al., Astrophys. J. **336**, L55 (1989).
  - [3] C. Rolfs and W. S. Rodney, Cauldrons in the Cosmos (University of Chicago, Chicago, 1988).
  - [4] C. Spitaleri, et al., Phys. Rev. C. **69**, 055806 (2004).
  - [5] L. Lamia, et al., Astrophys. J. **811**, 99 (2015).
  - [6] C. Spitaleri, et al., Phys. Rev. C. **63**, 055801 (2001).
  - [7] S. Romano, et al., Phys. J. A, **27**, 221 (2000).
  - [8] F. Raiola, et al., Eur. Phys. J. A. **13**, 377-382 (2002).
  - [9] M. Aliotta, et al., Eur. Phys. J. A. **9**, 435-437 (2000).
  - [10] A. Azhari, et al., Phys. Rev. C. **63**, 055803 (2001).
  - [11] S. Typel and G. Baur. Annals Phys. **305**, 288-265(2003).
  - [12] C. Spitaleri, et al., Phys.Lett.B. **755**,275-278 (2016).
  - [13] G. Baur. Phys.Lett.B. **178**, 135-138 (1986).
  - [14] F. Raiola,et al., Phys.Lett.B. **547**, 193-199 (2002).
  - [15] F. Strieder,et al., Sci. Nat. **88**, 461-467 (2001).
  - [16] F. Aliotta,et al., Nucl. Phys. A. **690**, 790 (2001).
  - [17] M. La Cognata, et al., Phys. Rev. C . **109**, 232701(2012).
  - [18] C. B. Li, et al., Phys. Rev. C . **95**, 035804 (2017).
  - [19] Q. G. Wen, et al., Phys. Rev. C . **93**, 035803(2016).
  - [20] Q. G. Wen, et al., Phys. Rev. C . **78**, 035805(2008).
  - [21] C. B. Li, et al., Nucl.Phys. Rev . **37**, 626-635(2020).
  - [22] A. J. Sierk and T. A. Tombrello. Nucl. Phys. A. **210**,341 (1973).
  - [23] D. Zahnow, et al., Z. Phys. A. **359**, 211 (1997).
  - [24] F. Kaihong, et al., Phys. Lett. B. **101**, 024310 (2018).